

UC San Diego

UC San Diego Previously Published Works

Title

Nexilin Is a New Component of Junctional Membrane Complexes Required for Cardiac T-Tubule Formation

Permalink

<https://escholarship.org/uc/item/4vv1k6mm>

Journal

Circulation, 140(1)

ISSN

0009-7322

Authors

Liu, Canzhao

Spinozzi, Simone

Chen, Jia-Yu

et al.

Publication Date

2019-07-02

DOI

10.1161/circulationaha.119.039751

Peer reviewed



Published in final edited form as:

Circulation. 2019 July 02; 140(1): 55–66. doi:10.1161/CIRCULATIONAHA.119.039751.

Nexilin is a New Component of Junctional Membrane Complexes Required for Cardiac T-tubule Formation

Canzhao Liu, MD, PhD^{1,*}, Simone Spinozzi, PhD^{1,*}, Jia-Yu Chen, PhD², Xi Fang, PhD¹, Wei Feng, MD, PhD¹, Guy Perkins, PhD³, Paola Cattaneo, PhD^{4,5}, Nuno Guimarães-Camboa, PhD^{6,7}, Nancy D. Dalton, RDCS¹, Kirk L. Peterson, MD¹, Tongbin Wu, PhD¹, Kunfu Ouyang, PhD⁸, Xiang-Dong Fu, PhD^{2,9}, Sylvia M. Evans, PhD^{1,10}, Ju Chen, PhD¹

¹Department of Medicine, University of California San Diego, La Jolla, CA 92093, USA.

²Department of Cellular and Molecular Medicine, University of California San Diego, La Jolla, CA 92093, USA.

³National Center for Microscopy and Imaging Research, University of California San Diego, La Jolla, CA 92093, USA.

⁴National Research Council, Institute of Genetics and Biomedical Research, Milan 20138, Italy.

⁵Humanitas Clinical and Research Center, Rozzano 20089, Italy.

⁶Institute for Cardiovascular Regeneration, Centre of Molecular Medicine, Goethe University Frankfurt, 60590 Frankfurt, Germany.

⁷German Center for Cardiovascular Research DZHK, Berlin 13347, Germany.

⁸Drug Discovery Center, State Key Laboratory of Chemical Oncogenomics, School of Chemical Biology and Biotechnology, Peking University Shenzhen Graduate School, Shenzhen 518055, China.

⁹Institute of Genomic Medicine, University of California San Diego, La Jolla, CA 92093, USA.

¹⁰Department of Pharmacology, Skaggs School of Pharmacy and Pharmaceutical Sciences, University of California San Diego, La Jolla, CA 92093, USA.

Abstract

Background: Membrane contact sites (MCS) are fundamental for transmission and translation of signals in multicellular organisms. A prime example is junctional membrane complexes (JMC) in the cardiac dyads, where T-tubules are juxtaposed to the sarcoplasmic reticulum (SR). T-tubule uncoupling and remodeling are well-known features of cardiac disease and heart failure. Even subtle alterations in the association between T-tubules and the Junctional SR can cause serious

Corresponding Author: Ju Chen, Ph.D. UCSD School of Medicine, BRF2 2A14, 9500 Gilman Drive, La Jolla, CA 92093-0613C, Phone: 858 822 4276; Fax: 858 822 3027, juchen@ucsd.edu.

*These authors contributed equally to this work and are listed in alphabetical order.

Author contributions: CL, SS, and JC designed the study. CL, SS, XF, WF, GP, PC, NGC, NDD, TW, and KF performed the research. CL, SS, JYC, XF, WF, GP, PC, NGC, NDD, KLP, TW, KF, XDF, SME, and JC analyzed and interpreted the data. CL, SS., SE, and JC wrote the manuscript.

Disclosures

None

cardiac disorders. Nexilin (NEXN) has been identified as an actin-binding protein and multiple mutations in the *NEXN* gene are associated with cardiac diseases, but the precise role of NEXN in heart function and disease is still unknown.

Methods: *Nexn* global and cardiomyocyte specific KO mice were generated. Comprehensive phenotypic and RNA-seq and mass spectrometry analyses were performed. Heart tissue samples and isolated single cardiomyocytes were analyzed by electron and confocal microscopy.

Results: Global and cardiomyocyte specific loss of *Nexn* in mice resulted in a rapidly progressive dilated cardiomyopathy. *In vivo* and *in vitro* analyses revealed that NEXN interacted with junctional SR proteins, was essential for optimal calcium transients, and was required for initiation of T-tubule invagination and formation.

Conclusion: These results demonstrated that NEXN is a pivotal component of the JMC, and is required for initiation and formation of T-tubules, thus providing insight into mechanisms underlying cardiomyopathy in patients with mutations in *NEXN*.

Keywords

Cardiomyopathy; T-Tubule; Membrane Contact Sites; Junctional Membrane Complexes

Introduction

Recent findings have highlighted the critical role of membrane contact sites (MCSs), regions of close apposition between membranes of distinct intracellular organelles, in mediating intra-organelle communication, upending the traditional view of intracellular organelles floating freely within the cytoplasm like boats in a pond¹⁻³. It has become progressively clear that endoplasmic reticulum-plasma membrane (ER-PM) contact sites are crucial for many different biological processes involved in cell homeostasis and organismal health⁴⁻⁸.

In cardiomyocytes, specialized MCSs with an average gap size of 12nm between the plasma membrane (also known as sarcolemma in muscle cells) and the highly specialized endoplasmic reticulum (sarcoplasmic reticulum/SR), termed junctional membrane complexes (JMCs), are essential for calcium ion (Ca^{2+})-induced Ca^{2+} release (CICR), an amplification of Ca^{2+} signaling required to generate and maintain the rhythmic contraction of the heart⁹⁻¹². In fetal cardiomyocytes the formation of the JMCs is dependent on the junctional protein Junctophilin2 (Jph2)¹³. In adult cardiomyocytes, amplification of Ca^{2+} release is possible owing to a highly specialized network of sarcolemmal invaginations, Transverse (T)-tubules that are closely associated with the SR in a dyad configuration¹⁴. CICR occurs when sarcolemmal depolarization activates L-type calcium channels (LTCCs), causing an influx of Ca^{2+} that triggers a much higher Ca^{2+} release from the SR via type 2 Ryanodine Receptors (RyR2s)⁹. In cardiomyocytes, these highly specialized JMCs, composed of clusters of LTCCs in the T-tubules, and RyR2 on the junctional SR are specifically localized in the dyads^{15, 16}. Optimal CICR requires proper formation of dyads and association of other regulatory proteins with LTCC and RyR2. The dyads of the adult cardiomyocyte are formed gradually during development in a highly orchestrated manner¹⁷. Seminal to dyad establishment, T-tubule formation is initiated around postnatal day 5 (P5),

as portions of the sarcolemma enriched in LTCC start to invaginate to become closely associated with the RyR2-enriched SR.

T-tubule uncoupling and remodeling are well-known features of cardiac disease and heart failure¹⁸⁻²². Even subtle alterations in the association between T-tubules and the Junctional SR can cause serious cardiac disorders²³. Despite the key role of T-tubule and SR coupling for cardiac function, proteins required to initiate T-tubule formation are unknown. Here, we identify Nexilin (NEXN) as a previously unsuspected component of the JMC and show that it is essential for initiating the sarcolemma invaginations that lead to T-tubule formation in postnatal cardiomyocytes.

Multiple mutations in *NEXN* are associated with cardiomyopathy in humans, and deficiency of NEXN in zebrafish results in perturbed Z-disk stability and heart failure, highlighting a significant role in cardiac function^{24, 25}. Global loss of NEXN in mice leads to severe cardiomyopathy and a reported endomyocardial fibroelastosis, resulting in perinatal death²⁶. In contradiction to the zebrafish model, no sarcomeric alterations in cardiomyocytes of *Nexn* global knockout (gKO) mice were noted²⁶. However, little is known as to specific role(s) of NEXN in cardiomyocytes, or mechanism(s) by which loss of NEXN results in rapidly progressive cardiomyopathy. Here, our findings reveal that NEXN, rather than being a Z-disk protein as previously thought, interacts with SR proteins and is required for initiation of T-tubule invagination and overall T-tubule formation. Our results demonstrate that NEXN is required to form this structure that is critical for optimal contraction of cardiomyocytes and normal heart function.

Methods

The data, analytical methods, and study materials will be made available to other researchers for the purposes of reproducing the results or replicating the procedure. The sources of reagents and detailed methods and any associated references are provided in the online-only Data Supplement. List of primers and antibodies used are reported in Supplemental Tables 1 and 2. All animal studies were performed in accordance with the NIH Guide for the Care and Use of Laboratory Animals²⁷ and approved by the Institutional Animal Care and Use Committee of the University of California, San Diego. The mouse line was generated as previously described (Supplemental Figure 1)²⁸. Neonatal and adult mice cardiomyocytes were prepared as previously described^{29, 30}. RNA-seq reads were mapped against the Ensembl v91 mouse gene model (GRCm38) for counting reads and estimating gene expression as described by Salmon³¹. The DEseq2 package³² was used to evaluate the reproducibility and perform differential gene expression analysis.

Statistics

The survival of *Nexn* mice was estimated using the Kaplan-Meier method, and survival curves were compared using the log-rank test. For all other statistics, values were expressed as mean \pm SEM and statistical differences were tested by 2-tailed Student's t-test. A value of $P < 0.05$ was considered statistically significant. All the analyses were performed with GraphPad Prism software.

Results

Cardiomyocyte specific ablation of *Nexn* results in a rapidly progressive severe dilated cardiomyopathy

To investigate the role of NEXN in cardiac function, we generated *Nexn* gKO mice by crossing targeted mice containing *Nexn* floxed alleles (*Nexn^{f/f}*) with global deleter *Sox2-cre* mice, resulting in complete loss of the protein (Supplemental Figure 1A-C). Global deficiency of NEXN resulted in perinatal lethality. All *Nexn* gKO mice died before postnatal day 12 (P12) exhibiting decreased body weight starting at 5 days after birth (P5). Heart weight to body weight (HW/BW) and heart weight to tibial length (HW/TL) ratios were significantly increased in gKO mice compared to WT littermate controls (CTRL) starting from P5 (Supplemental Figure 1D-F).

Transthoracic echocardiography revealed that global loss of NEXN resulted in increased left ventricular diameter (Supplemental Figure 1H, I). Abnormal dimensions in the heart were accompanied by reduced systolic cardiac function, as evidenced by a significant decrease in fractional shortening percentage (%FS) in *gKO* mice. Although left ventricular dimensions in *Nexn* gKO mice were not significantly changed compared to CTRLs at postnatal day 1 (P1), %FS was already reduced by 20% (Supplemental Figure 1G). To determine the starting point of abnormal heart function, echocardiography at embryonic day 18.5 (E18.5) mice was performed. No significant changes in %FS were observed between *Nexn^{-/-}* mice and WT littermates at E18.5 (Supplemental Figure 1G), indicating that defects in heart function consequent to loss of NEXN began to develop after E18.5.

Gross anatomical characterization of KO mice confirmed severe cardiac enlargement starting from P5 (Supplemental Figure 1J). Histological analysis of gKO hearts showed severe left ventricular dilation starting from P5 with a progressive phenotype, leading to thinning of the cardiac walls, clearly visible at postnatal day 10 (P10) (Supplemental Figure 1K).

Aherrahrou and colleagues reported that dilated hearts from *Nexn* gKO mice evidence endomyocardial fibroelastosis, a thickening of the endocardium characterized by elastic fibers and collagen²⁶. Although we similarly observed, from P7 onward, collagen positive “mural masses” in left ventricles of *Nexn* gKO mice, further histological analyses revealed an absence of elastic fibers, and presence of fibrin in these structures, suggesting they were most likely intracardiac mural thrombi (Supplemental Figure 2, Supplemental Movie).

To confirm that the *Nexn* gKO cardiac phenotype resulted from specific loss of NEXN in cardiomyocytes, we crossed *Nexn^{f/f}* mice with cardiomyocyte-specific *Xenopus laevis* myosin light-chain 2-Cre (XMLC2) transgenic mice³³. This XMLC2-Cre line specifically drives Cre recombinase activity in myocardial cells (Supplemental Figure 3), our echocardiography studies also showed that this XMLC2-Cre mouse line in the same genetic background as that of our mouse models has normal cardiac function (Supplemental Figure 4). All *Nexn* cardiomyocytes specific KO (cKO) mice died before P12, with phenotypes recapitulating those of gKOs (Fig. 1, 2; Supplemental Table 3). Thus, reduced body size and weight, altered cardiac function, and resulting dilated cardiomyopathy (DCM) were all a

direct consequence of NEXN loss in cardiomyocytes. Similar results were also obtained crossing *Nexn*^{f/f} mice to cardiomyocyte-specific troponin T2 (cTNT) cre transgenic mice (Supplemental Figure 5).

Loss of Nexilin alters Ca²⁺-handling gene and protein expression in the heart

To gain a better understanding of how loss of NEXN in cardiomyocytes leads to this rapidly progressing severe DCM, we constructed RNA-Sequencing (RNA-Seq) libraries from cardiac ventricles of mice at P1, a time prior to *Nexn* cKO mice develop DCM and found that 74 genes were significantly altered in *Nexn* cKOs (Supplemental Figure 6, Fig. 3A). Gene Ontology (GO) enrichment analysis identified the top biological processes or molecular functions as extracellular structure organization, heart development, and Ca²⁺-binding (Fig. 3B). Quantitative PCR (q-PCR) on samples from hearts of E18.5 mice confirmed that expression of a set of Ca²⁺-handling proteins was altered in *Nexn* cKO mice with respect to littermate CTRLs, suggesting SR stress. Among these genes, calsequestrin, the main Ca²⁺-buffering protein of the SR, were significantly upregulated (Fig. 3C). To further investigate possible involvement of Ca²⁺-handling machinery in the phenotype resulting from cardiomyocyte-specific ablation of *Nexn*, we also performed mass spectrometry on lysates from P1 cardiac ventricles. A total of 2456 proteins were identified and quantified, with NEXN itself showing the most significant fold-change (Fig. 3D), suggesting the feasibility of this strategy for identifying changes at the proteome level. 185 proteins were substantially altered in cKO hearts compared to those of CTRLs (Fig. 3D). Consistent with results from RNA-seq, GO term enrichment analysis revealed proteins involved primarily in regulation of muscle system (Fig. 3E), including 12 Ca²⁺-binding proteins (Supplemental Table 4).

To investigate whether observed altered levels in Ca²⁺-binding proteins detected at P1 in *Nexn* cKO hearts could be a primary cause leading to DCM, western blot analyses for some of the major Ca²⁺-related proteins was performed on lysates from E18.5 hearts, a time just prior to evident defects in cardiac function. Results demonstrated that RyR2, LTCC subunits *Cacna1c* and *Cacna2d1*, *Serc2*, and *Casq1* had altered expression levels in cKO hearts relative to those in CTRLs (Fig. 3F, G). Interestingly, although mRNA levels of *Casq2*, the major calsequestrin isoform in the heart, were slightly upregulated, its protein levels were not changed (Supplemental Figure 7) To further demonstrate that abnormal Ca²⁺-handling protein expression preceded functional and structural changes in *Nexn* cKOs, an *in vitro* model of acute *Nexn* ablation was utilized, treating primary neonatal *Nexn*^{f/f} cardiomyocytes with a Cre-expressing adenovirus. Subsequent western blot analyses revealed changes in Ca²⁺-handling proteins consistent with those obtained from E18.5 ventricles (Fig. 3H, I). These results suggested a mechanistic link between Ca²⁺-handling and DCM caused by loss of NEXN.

Nexilin is crucial for Ca²⁺ homeostasis in cardiomyocytes

To determine functional consequences of altered Ca²⁺-handling gene and protein expression, we tested Ca²⁺ flux in cardiomyocytes isolated from E18.5 *Nexn* cKO mice and littermate CTRLs stained with the Fluo4 Ca²⁺ indicator. Results from time-lapse confocal microscopy showed that the amplitude of Ca²⁺-transients was significantly reduced, and the decay of the

Ca²⁺ transient (Tau) was slower in cKO cardiomyocytes (Fig. 4A-E). Since alterations in Ca²⁺ transients can either be a cause or consequence of heart failure³⁴, we also studied Ca²⁺ transients in cardiomyocytes following acute loss of NEXN. Cardiomyocytes were isolated from E18.5 *Nexn*^{f/f} mice and transfected with adenovirus expressing Cre (Ad-Cre) or control adenovirus expressing LacZ (Ad-LacZ). 24 hours following transfection, cells were stained with Fluo4 and time-lapse confocal imaging performed. Similar to results obtained with *Nexn* cKO cardiomyocytes, Ca²⁺ transients in Ad-Cre *Nexn*^{f/f} cardiomyocytes were reduced in amplitude, had increased duration, and prolonged decay relative to control Ad-LacZ *Nexn*^{f/f} cardiomyocytes (Fig. 4F-J). These data supported the hypothesis that aberrant Ca²⁺-homeostasis in cKO cardiomyocytes was most likely the cause, and not a consequence of subsequently reduced cardiac output and progressive DCM.

Nexilin is a newly identified component of junctional membrane complexes in the cardiac dyad

NEXN has been characterized in previous studies as a Z-disc protein and loss of NEXN in zebrafish results in perturbed Z-disc stability²⁴. However, more recently it has been reported that gKO of *Nexn* in mice does not alter sarcomere integrity or Z-disc structure²⁶. Likewise, in our gKO and cKO models, these structures were not altered (Supplemental Figure 8A). In adult heart, the terminal cisternae of the SR and T-tubules are localized to the Z-disc³⁵, and we observed abnormal Ca²⁺-homeostasis in *Nexn* cKO cardiomyocytes. Following upon these observations, we decided to further investigate NEXN's precise localization in cardiomyocytes, and its potential association with dyad proteins. To do this, we generated three antibodies from three different epitopes. One of these antibodies, generated utilizing a peptide encoded by exon 6, included in all NEXN isoforms, exhibited a signal in wildtype, but not cKO tissue, either by western blot or by immunofluorescence (Supplemental Figure 1C, Supplemental Figure 8B). Utilizing this antibody, confocal microscopy revealed that NEXN co-localized with the junctional SR protein Jph2 in both isolated neonatal cardiomyocytes (when the Z-disc is already formed, but T-tubules and junctional SR are not) and adult cardiomyocytes (when mature T-tubules and junctional SR localize along the Z-discs), (Fig. 5A, B).

In further support of NEXN being localized to the JMC, western blot analyses of proteins co-immunoprecipitated with NEXN from mouse heart lysates identified two major junctional SR proteins (RyR2, Jph2), as possible binding partners of NEXN (Fig. 5C). Actin was also co-immunoprecipitated with NEXN, consistent with previous studies³⁶, but T-tubule proteins Cacna2d1 and Bin1, or the major Z-line protein alpha actinin, were not co-immunoprecipitated with NEXN. To further validate these associations, we co-expressed GFP-tagged NEXN and Flag-tagged Jph2 in HEK293 cells and expressed GFP-tagged NEXN in a stable tetracycline inducible RyR2-expressing HEK293 cell line³⁷ and performed pull-down experiments on cell protein extracts. Western blot analyses of pull-down results confirmed that NEXN was co-immunoprecipitated with both Jph2 and RyR2 (Fig. 5D, E). Western blot analyses also demonstrated that levels of Jph2, but not Bin1, were significantly reduced both in *Nexn* cKO heart tissue samples, and in the *in vitro* model of acute *Nexn* ablation (Fig. 5F-I). These findings indicated that NEXN was not a Z-disc protein and its localization at the JMC reflected its association with junctional SR-proteins.

Nexilin is essential for initiation of cardiac T-tubule formation

Considering NEXN association with JMC proteins, abnormal junctional protein expression and impaired Ca^{2+} transients in *Nexn* cKO cardiomyocytes, we investigated T-tubule morphology. Cardiomyocytes were isolated from *Nexn* cKO and littermate CTRL mice at P5 and P10 and stained them with the T-tubule marker Di-8-ANNEPS²⁰. Live-imaging confocal microscopy showed that membrane invaginations typical of initial T-tubule formation were evident in P5 CTRL cardiomyocytes but were not observed in *Nexn* cKO cardiomyocytes (Fig. 6A). Furthermore, in contrast to CTRL samples, organized T-tubules were completely absent in P10 *Nexn* cKO cardiomyocytes (Fig. 6B). We also analyzed formation of peripheral junctional membrane complexes at E18.5. At this stage, two types of peripheral SR/Sarcolemma associations are present, one separated by a space of 30nm (when the junctional membrane complex is forming), and the other by a space of 12nm (when the junctional membrane complex is established)¹³. Electron microscopy analyses showed that in E18.5 *Nexn* cKO cardiomyocytes, when compared to CTRLS, 12nm junctions were significantly decreased, while 30nm junctions were significantly increased (Fig. 6C-E). These findings suggested impaired associations between the SR and sarcolemma, and failure of sarcolemmal invaginations required to initiate T-tubule formation in *Nexn* cKO cardiomyocytes.

Discussion

Mutations in *NEXN* are associated with cardiomyopathies and a first animal model in zebrafish suggested NEXN as a sarcomeric protein localized to the Z-disc and involved in its stability^{24, 25}. More recently, Aherrahrou and colleagues reported that global KO of *Nexn* in mice did not alter sarcomeric structure of cardiomyocytes, but resulted in severe DCM, with aspects of endocardial fibroelastosis²⁶. Here, similarly, we found that *Nexn*^{-/-} mice developed a severe, progressive DCM, with cardiac dysfunction first evident at P1, and collagen positive “mural masses” evident by P7. However, absence of elastic fibers and presence of fibrin suggested these masses were thrombi, rather than endocardial fibroelastosis. Considering the early onset of DCM against the later onset of the thrombi, the latter could not be considered a primary cause of altered cardiac function (Supplemental Figure 1, 2). We found that cKO of *Nexn* in cardiomyocytes totally recapitulated phenotypes observed in *Nexn*^{-/-} mice (Fig. 1, 2), demonstrating that the DCM was a direct consequence of NEXN loss in cardiomyocytes.

Investigating mechanisms underlying cardiac dysfunction in *Nexn* cKO mice, mass spectrometry and western blot analysis of cardiac extracts showed that loss of NEXN resulted in altered expression of Ca^{2+} -handling proteins such as RyR2, the LTCC pore-forming subunit *Cacna1c*, and *Jph2*. These data were confirmed utilizing an in vitro model of acute NEXN loss (Fig. 3). Consistent with these observations, loss of NEXN in cardiomyocytes resulted in abnormal Ca^{2+} transients, characterized by reduced amplitude, increased duration, and prolonged decay with respect to those of CTRLs (Fig. 4). *Nexn* cKO mice also exhibited diminished cardiac contractility and rapidly progressive cardiomyopathy and died before P12. Abnormal expression of SR proteins and changes in Ca^{2+} transients are manifestations of defects in EC-coupling and a hallmark of cardiac JMC dysfunction^{38, 39},

suggesting a potential role for NEXN in the specialized SR/T-tubule association necessary for dyad formation.

Development of the dyads of the adult cardiomyocyte occurs in a gradual, highly orchestrated manner. At embryonic day 9 (E9), early associations between the sarcolemma and ER membranes with gap sizes of either 12nm or 30 nm are progressively observed at the cell periphery¹³. At perinatal stages, newly formed SR cisternae enriched in RyR2 at the cell periphery are periodically arranged in association with the Z-disc^{40, 41}. Around postnatal day 5 (P5), initiation of T-tubule formation occurs, as portions of the sarcolemma enriched in LTCC start to invaginate to become closely associated with the RyR2-enriched SR. From P10, these sarcolemmal invaginations penetrate more deeply within the cytoplasm, forming mature T-tubules that are juxtaposed to the junctional SR with an average gap size of 12nm, likely reflecting a requisite distance for physiological cross-talk between LTCCs and RyR2s¹³.

Proper dyad formation is essential for cardiac function, with even subtle alterations in association between T-tubules and the Junctional SR causing serious cardiac disorders²³. However, we know relatively little as to proteins orchestrating the development of this highly specialized architecture. Initial formation of early ER-PM associations requires the transmembrane ER/SR protein Jph2^{42, 43}, as global deficiency of Jph2 results in 90% loss of the 12nm ER-PM associations at E9.5, with mutants dying around E10.5¹³. In mature cardiomyocytes, T-tubule architecture is modified by bridging integrator 1 (Bin1). In cardiomyocyte-specific Bin1 mutants, T-tubule distribution is not changed, but individual T-tubules exhibit fewer folds and overall less membrane content, resulting in susceptibility to arrhythmias in adult mice⁴⁴.

Although initiation of T-tubule development is a pivotal moment in mature dyad development, little is known as to proteins required for this key event. Here, we demonstrated through a series of observations that NEXN was a JMC protein required for initiation of T-tubule development. Immunostaining with an antibody specific to NEXN at P5 demonstrated that NEXN co-localized with Jph2 at the periphery, but was not present throughout the Z-disc, as observed for the Z-disc protein α -actinin (Fig. 5), suggesting that NEXN localized in the forming JMC and was not a Z-disc protein. Consistent with this, proteomics and pull-down assays demonstrated that NEXN interacted with junctional SR proteins Jph2 and RyR2 (Fig. 5C-E). Confocal analyses at P5 and P10 demonstrated that loss of NEXN in cardiomyocytes resulted in absence of sarcolemmal invaginations required to initiate T-tubule formation, and lack of T-tubule formation (Fig. 6A, B). It should also be pointed out that, although we did not detect alterations in JPH2 immunostaining by confocal microscopy in NEXN P5 cKO cardiomyocytes (Supplemental Figure 8), implying normal SR structure, more in depth studies would be required to unequivocally determine whether SR structures were changed in cKO cardiomyocytes.

Our data suggests a model in which NEXN is critical for two aspects of JMC formation in cardiomyocytes. At E18.5, relative to CTRLs, *Nexn* mutant cardiomyocytes exhibited a reduced proportion of the more closely apposed 12nm associations between the ER and sarcolemma at the cell periphery (Fig. 7). At P5, NEXN mutants failed to develop

sarcolemmal invaginations initiating T-tubule development, resulting in absence of T-tubule development at P10 (Fig. 7).

Altogether, results presented in this study identify NEXN as an unexpected component of JMCs in cardiomyocytes that is essential for T-tubule initiation and formation. Furthermore, our studies given mechanistic insight into molecular pathways leading to cardiomyopathy in patients with mutations in *NEXN*. It remains to be determined whether NEXN also plays a central role in T-tubule/JMC remodeling during heart failure. Of note, NEXN protein levels are not significantly altered in human cardiomyopathy or heart failure patients⁴⁵, or in mouse heart two weeks following TAC (Supplemental Figure 9). However, these observations do not exclude an essential role of NEXN in T-tubule/JMC remodeling during heart failure. In fact, protein levels of RyR2, a major JMC protein and an interacting partner of NEXN, are also not altered in heart failure, but RyR2 function is significantly diminished due to post translational modifications⁴⁶⁻⁴⁸. Further studies are needed to determine the potential role of NEXN in T-tubule/JMC remodeling during heart failure, and whether NEXN may have roles other than T-tubule/JMC formation.

Supplementary Material

Refer to Web version on PubMed Central for supplementary material.

Acknowledgments

We thank Dr. Paolo Toti, (UNISI, Siena, Italy), Dr. Michael C. Fishbein (UCLA, Los Angeles, CA, USA) and Dr. Robert Ross (UCSD, La Jolla, CA, USA) for outstanding scientific discussions on histology results. We are grateful for their invaluable technical assistance to Dr. Alex Rosa Campos (SBP Proteomics Core of UCSD, La Jolla, CA, USA), Dr. Tea Jashashvili (MIC of USC, Los Angeles, CA, USA), Dr. Jennifer Santini (Microscopy Core of UCSD, La Jolla, CA, USA), Dr. Mark Ellisman and all the members of NCMIR (UCSD, La Jolla, CA, USA). We also thank Dr. Chao Chen and Dr. Robert Ross (UCSD, La Jolla, CA, USA) for providing the Cre-adenoviral vector used for the in vitro acute loss of Nexn. We thank Dr. Adam Pollak (UCSD, La Jolla, CA, USA) and Dr. S. R. Wayne Chen (University of Calgary, Canada) for the tetracycline inducible Ryr2-expressing HEK293 cell line.

Sources of Funding:

JC is funded by grants from NIH, the National Heart, Lung, and Blood Institute and holds an American Heart Association Endowed Chair in Cardiovascular Research. XF is supported by a NIH grant K99HL143210. OK is supported by the Shenzhen Basic Research Foundation (KCYJ20160428154108239, KQJSCX20170330155020267). We also thank National Center for Microscopy and Imaging Research grant support: 5P41GM103412 to Mark Ellisman.

References

1. Prinz WA. Bridging the gap: membrane contact sites in signaling, metabolism, and organelle dynamics. *J Cell Biol.* 2014;205:759–769. [PubMed: 24958771]
2. Valm AM, Cohen S, Legant WR, Melunis J, Hershberg U, Wait E, Cohen AR, Davidson MW, Betzig E and Lippincott-Schwartz J. Applying systems-level spectral imaging and analysis to reveal the organelle interactome. *Nature.* 2017;546:162–167. [PubMed: 28538724]
3. Helle SC, Kanfer G, Kolar K, Lang A, Michel AH and Kornmann B. Organization and function of membrane contact sites. *Biochim Biophys Acta.* 2013;1833:2526–2541. [PubMed: 23380708]
4. Giordano F, Saheki Y, Idevall-Hagren O, Colombo SF, Pirruccello M, Milosevic I, Gracheva EO, Bagriantsev SN, Borgese N and De Camilli P. PI(4,5)P(2)-dependent and Ca(2+)-regulated ER-PM interactions mediated by the extended synaptotagmins. *Cell.* 2013;153:1494–1509. [PubMed: 23791178]

5. Lees JA, Messa M, Sun EW, Wheeler H, Torta F, Wenk MR, De Camilli P and Reinisch KM. Lipid transport by TMEM24 at ER-plasma membrane contacts regulates pulsatile insulin secretion. *Science*. 2017;355:709.
6. Stefan CJ, Manford AG, Baird D, Yamada-Hanff J, Mao Y and Emr SD. Osh proteins regulate phosphoinositide metabolism at ER-plasma membrane contact sites. *Cell*. 2011;144:389–401. [PubMed: 21295699]
7. Caldieri G, Barbieri E, Nappo G, Raimondi A, Bonora M, Conte A, Verhoef L, Confalonieri S, Malabarba MG, Bianchi F, Cuomo A, Bonaldi T, Martini E, Mazza D, Pinton P, Tacchetti C, Polo S, Di Fiore PP and Sigismund S. Reticulon 3-dependent ER-PM contact sites control EGFR nonclathrin endocytosis. *Science*. 2017;356:617–624. [PubMed: 28495747]
8. Phillips MJ and Voeltz GK. Structure and function of ER membrane contact sites with other organelles. *Nat Rev Mol Cell Biol*. 2016;17:69–82. [PubMed: 26627931]
9. Bers DM. Cardiac excitation-contraction coupling. *Nature*. 2002;415:198–205. [PubMed: 11805843]
10. Endo M Calcium-induced calcium release in skeletal muscle. *Physiol Rev*. 2009;89:1153–1176. [PubMed: 19789379]
11. Berridge MJ, Bootman MD and Roderick HL. Calcium signalling: dynamics, homeostasis and remodelling. *Nat Rev Mol Cell Biol*. 2003;4:517–529. [PubMed: 12838335]
12. Venetucci L, Denegri M, Napolitano C and Priori SG. Inherited calcium channelopathies in the pathophysiology of arrhythmias. *Nat Rev Cardiol*. 2012;9:561–575. [PubMed: 22733215]
13. Takeshima H, Komazaki S, Nishi M, Iino M and Kangawa K. Junctophilins: a novel family of junctional membrane complex proteins. *Mol Cell*. 2000;6:11–22. [PubMed: 10949023]
14. Scriven DR, Asghari P and Moore ED. Microarchitecture of the dyad. *Cardiovasc Res*. 2013;98:169–176. [PubMed: 23400762]
15. Franzini-Armstrong C, Protasi F and Ramesh V. Shape, size, and distribution of Ca(2+) release units and couplons in skeletal and cardiac muscles. *Biophys J*. 1999;77:1528–1539. [PubMed: 10465763]
16. Song LS, Sobie EA, McCulle S, Lederer WJ, Balke CW and Cheng H. Orphaned ryanodine receptors in the failing heart. *Proc Natl Acad Sci U S A*. 2006;103:4305–4310. [PubMed: 16537526]
17. Louch WE, Koivumaki JT and Tavi P. Calcium signalling in developing cardiomyocytes: implications for model systems and disease. *J Physiol*. 2015;593:1047–1063. [PubMed: 25641733]
18. Zhang HB, Li RC, Xu M, Xu SM, Lai YS, Wu HD, Xie XJ, Gao W, Ye H, Zhang YY, Meng X and Wang SQ. Ultrastructural uncoupling between T-tubules and sarcoplasmic reticulum in human heart failure. *Cardiovasc Res*. 2013;98:269–276. [PubMed: 23405000]
19. Wei S, Guo A, Chen B, Kutschke W, Xie YP, Zimmerman K, Weiss RM, Anderson ME, Cheng H and Song LS. T-tubule remodeling during transition from hypertrophy to heart failure. *Circ Res*. 2010;107:520–531. [PubMed: 20576937]
20. Wagner E, Lauterbach MA, Kohl T, Westphal V, Williams GS, Steinbrecher JH, Streich JH, Korff B, Tuan HT, Hagen B, Luther S, Hasenfuss G, Parlitz U, Jafri MS, Hell SW, Lederer WJ and Lehnart SE. Stimulated emission depletion live-cell super-resolution imaging shows proliferative remodeling of T-tubule membrane structures after myocardial infarction. *Circ Res*. 2012;111:402–414. [PubMed: 22723297]
21. Xie YP, Chen B, Sanders P, Guo A, Li Y, Zimmerman K, Wang LC, Weiss RM, Grumbach IM, Anderson ME and Song LS. Sildenafil prevents and reverses transverse-tubule remodeling and Ca(2+) handling dysfunction in right ventricle failure induced by pulmonary artery hypertension. *Hypertension*. 2012;59:355–362. [PubMed: 22203744]
22. Zhang C, Chen B, Guo A, Zhu Y, Miller JD, Gao S, Yuan C, Kutschke W, Zimmerman K, Weiss RM, Wehrens XH, Hong J, Johnson FL, Santana LF, Anderson ME and Song LS. Microtubule-mediated defects in junctophilin-2 trafficking contribute to myocyte transverse-tubule remodeling and Ca2+ handling dysfunction in heart failure. *Circulation*. 2014;129:1742–1750. [PubMed: 24519927]
23. Lyon AR, MacLeod KT, Zhang Y, Garcia E, Kanda GK, Lab MJ, Korchev YE, Harding SE and Gorelik J. Loss of T-tubules and other changes to surface topography in ventricular myocytes from

- failing human and rat heart. *Proc Natl Acad Sci U S A.* 2009;106:6854–6859. [PubMed: 19342485]
24. Hassel D, Dahme T, Erdmann J, Meder B, Hüge A, Stoll M, Just S, Hess A, Ehlermann P, Weichenhan D, Grimm M, Liptau H, Hetzer R, Regitz-Zagrosek V, Fischer C, Nürnberg P, Schunkert H, Katus HA and Rottbauer W. Nexilin mutations destabilize cardiac Z-disks and lead to dilated cardiomyopathy. *Nat Med.* 2009;15:1281–1288. [PubMed: 19881492]
 25. Wang H, Li Z, Wang J, Sun K, Cui Q, Song L, Zou Y, Wang X, Liu X, Hui R and Fan Y. Mutations in NEXN, a Z-disc gene, are associated with hypertrophic cardiomyopathy. *Am J Hum Genet.* 2010;87:687–693. [PubMed: 20970104]
 26. Aherrahrou Z, Schlossarek S, Stoelting S, Klinger M, Geertz B, Weinberger F, Kessler T, Aherrahrou R, Moreth K, Bekeredjian R, Hrabe de Angelis M, Just S, Rottbauer W, Eschenhagen T, Schunkert H, Carrier L and Erdmann J. Knock-out of nexilin in mice leads to dilated cardiomyopathy and endomyocardial fibroelastosis. *Basic Res Cardiol.* 2016;111:6. [PubMed: 26659360]
 27. *Guide for the Care and Use of Laboratory Animals National Research Council National Academies Press, Washington, DC; 2011.*
 28. Liang X, Zhou Q, Li X, Sun Y, Lu M, Dalton N, Ross J Jr. and Chen J. PINCH1 plays an essential role in early murine embryonic development but is dispensable in ventricular cardiomyocytes. *Mol Cell Biol.* 2005;25:3056–3062. [PubMed: 15798193]
 29. Fang X, Stroud MJ, Ouyang K, Fang L, Zhang J, Dalton ND, Gu Y, Wu T, Peterson KL, Huang HD, Chen J and Wang N. Adipocyte-specific loss of PPAR γ attenuates cardiac hypertrophy. *JCI Insight.* 2016;1:e89908. [PubMed: 27734035]
 30. Fang X, Bogomolovas J, Wu T, Zhang W, Liu C, Veevers J, Stroud MJ, Zhang Z, Ma X, Mu Y, Lao DH, Dalton ND, Gu Y, Wang C, Wang M, Liang Y, Lange S, Ouyang K, Peterson KL, Evans SM and Chen J. Loss-of-function mutations in co-chaperone BAG3 destabilize small HSPs and cause cardiomyopathy. *J Clin Invest.* 2017;127:3189–3200. [PubMed: 28737513]
 31. Patro R, Duggal G, Love MI, Irizarry RA and Kingsford C. Salmon provides fast and bias-aware quantification of transcript expression. *Nat Methods.* 2017;14:417–419. [PubMed: 28263959]
 32. Love MI, Huber W and Anders S. Moderated estimation of fold change and dispersion for RNA-seq data with DESeq2. *Genome Biol.* 2014;15:550. [PubMed: 25516281]
 33. Breckenridge R, Kotecha S, Towers N, Bennett M and Mohun T. Pan-myocardial expression of Cre recombinase throughout mouse development. *Genesis.* 2007;45:135–144. [PubMed: 17334998]
 34. Lou Q, Janardhan A and Efimov IR. Remodeling of calcium handling in human heart failure. *Adv Exp Med Biol.* 2012;740:1145–1174. [PubMed: 22453987]
 35. Hong T and Shaw RM. Cardiac T-Tubule Microanatomy and Function. *Physiol Rev.* 2017;97:227–252. [PubMed: 27881552]
 36. Ohtsuka T, Nakanishi H, Ikeda W, Satoh A, Momose Y, Nishioka H and Takai Y. Nexilin: a novel actin filament-binding protein localized at cell-matrix adherens junction. *J Cell Biol.* 1998;143:1227–1238. [PubMed: 9832551]
 37. Jiang D, Xiao B, Yang D, Wang R, Choi P, Zhang L, Cheng H and Chen SR. RyR2 mutations linked to ventricular tachycardia and sudden death reduce the threshold for store-overload-induced Ca²⁺ release (SOICR). *Proc Natl Acad Sci U S A.* 2004;101:13062–13067. [PubMed: 15322274]
 38. Gorski PA, Ceholski DK and Hajjar RJ. Altered myocardial calcium cycling and energetics in heart failure—a rational approach for disease treatment. *Cell Metab.* 2015;21:183–194. [PubMed: 25651173]
 39. van Oort RJ, Garbino A, Wang W, Dixit SS, Landstrom AP, Gaur N, De Almeida AC, Skapura DG, Rudy Y, Burns AR, Ackerman MJ and Wehrens XH. Disrupted junctional membrane complexes and hyperactive ryanodine receptors after acute junctophilin knockdown in mice. *Circulation.* 2011;123:979–988. [PubMed: 21339484]
 40. Ziman AP, Gomez-Viquez NL, Bloch RJ and Lederer WJ. Excitation-contraction coupling changes during postnatal cardiac development. *J Mol Cell Cardiol.* 2010;48:379–386. [PubMed: 19818794]
 41. Korhonen T, Rapila R, Ronkainen VP, Koivumäki JT and Tavi P. Local Ca²⁺ releases enable rapid heart rates in developing cardiomyocytes. *J Physiol.* 2010;588:1407–1417. [PubMed: 20211983]

42. Guo A, Wang Y, Chen B, Wang Y, Yuan J, Zhang L, Hall D, Wu J, Shi Y, Zhu Q, Chen C, Thiel WH, Zhan X, Weiss RM, Zhan F, Musselman CA, Pufall M, Zhu W, Au KF, Hong J, Anderson ME, Grueter CE and Song LS. E-C coupling structural protein junctophilin-2 encodes a stress-adaptive transcription regulator. *Science*. 2018;362:1375.
43. Reynolds JO, Chiang DY, Wang W, Beavers DL, Dixit SS, Skapura DG, Landstrom AP, Song LS, Ackerman MJ and Wehrens XH. Junctophilin-2 is necessary for T-tubule maturation during mouse heart development. *Cardiovasc Res*. 2013;100:44–53. [PubMed: 23715556]
44. Hong T, Yang H, Zhang SS, Cho HC, Kalashnikova M, Sun B, Zhang H, Bhargava A, Grabe M, Olgin J, Gorelik J, Marban E, Jan LY and Shaw RM. Cardiac BIN1 folds T-tubule membrane, controlling ion flux and limiting arrhythmia. *Nat Med*. 2014;20:624–632. [PubMed: 24836577]
45. Chen CY, Caporizzo MA, Bedi K, Vite A, Bogush AI, Robison P, Heffler JG, Salomon AK, Kelly NA, Babu A, Morley MP, Margulies KB and Prosser BL. Suppression of deetyrosinated microtubules improves cardiomyocyte function in human heart failure. *Nat Med*. 2018;24:1225–1233. [PubMed: 29892068]
46. Sainte Beuve C, Allen PD, Dambrin G, Rannou F, Marty I, Trouve P, Bors V, Pavie A, Gandjbakch I and Charlemagne D. Cardiac calcium release channel (ryanodine receptor) in control and cardiomyopathic human hearts: mRNA and protein contents are differentially regulated. *J Mol Cell Cardiol*. 1997;29:1237–1246. [PubMed: 9160875]
47. Meyer M, Schillinger W, Pieske B, Holubarsch C, Heilmann C, Posival H, Kuwajima G, Mikoshiba K, Just H, Hasenfuss G and et al. Alterations of sarcoplasmic reticulum proteins in failing human dilated cardiomyopathy. *Circulation*. 1995;92:778–784. [PubMed: 7641356]
48. Schillinger W, Meyer M, Kuwajima G, Mikoshiba K, Just H and Hasenfuss G. Unaltered ryanodine receptor protein levels in ischemic cardiomyopathy. *Mol Cell Biochem*. 1996;160–161:297–302.

Clinical Perspective

What is new?

- Cardiomyocyte specific KO of *Nexn* results in a rapidly progressive severe dilated cardiomyopathy.
- NEXN interacts with SR proteins, and is a previously unsuspected member of the SR-sarcolemma junctional complex
- NEXN is required for initiation of T-tubule invagination and overall T-tubule formation, with loss of NEXN leading to impaired calcium handling.

What are the clinical implications?

- Identification of NEXN as a new possible target for T-Tubule remodeling.
- Providing mechanistic insight into molecular pathways leading to cardiomyopathy in patients with mutations in *NEXN*.

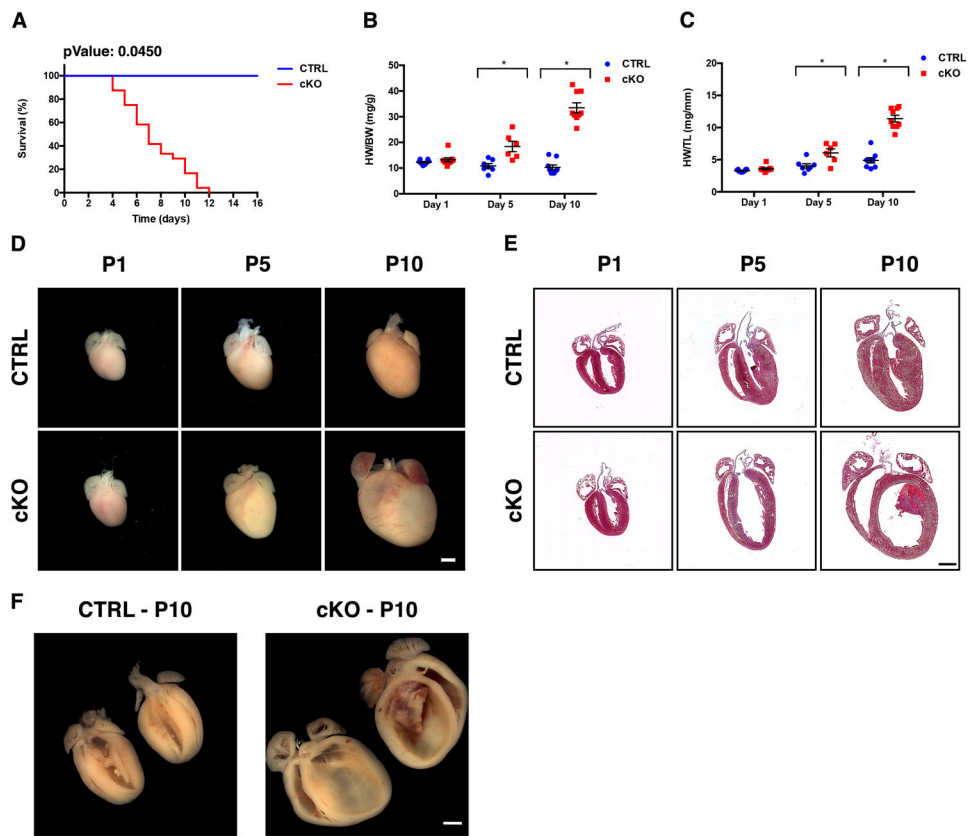


Figure 1. Loss of NEXN in cardiomyocytes results in a progressive dilated cardiomyopathy. (A) Kaplan-Meier survival curves for NEXN CTRL (n = 35) and cKO (n = 24) mice; (B, C) Graphs showing (B) HW/BW (n=7-9 mice per time point) and (C) HW/TL (n=5-6 mice per time point) in CTRL and cKO mice. (*) Statistically significant differences with P value < 0.05. (D) Representative whole heart images from postnatal day 1 (P1), 5 (P5) or 10 (P10) mice. (E) Representative 4-chambers view Masson's trichrome staining images of longitudinal histological sections from the same stages. (F) Butterfly cut gross anatomy showing the tridimensional organization of the organized thrombus in the left ventricle of the cKO heart and the relative CTRL. (D-F) Scale bars 1mm.

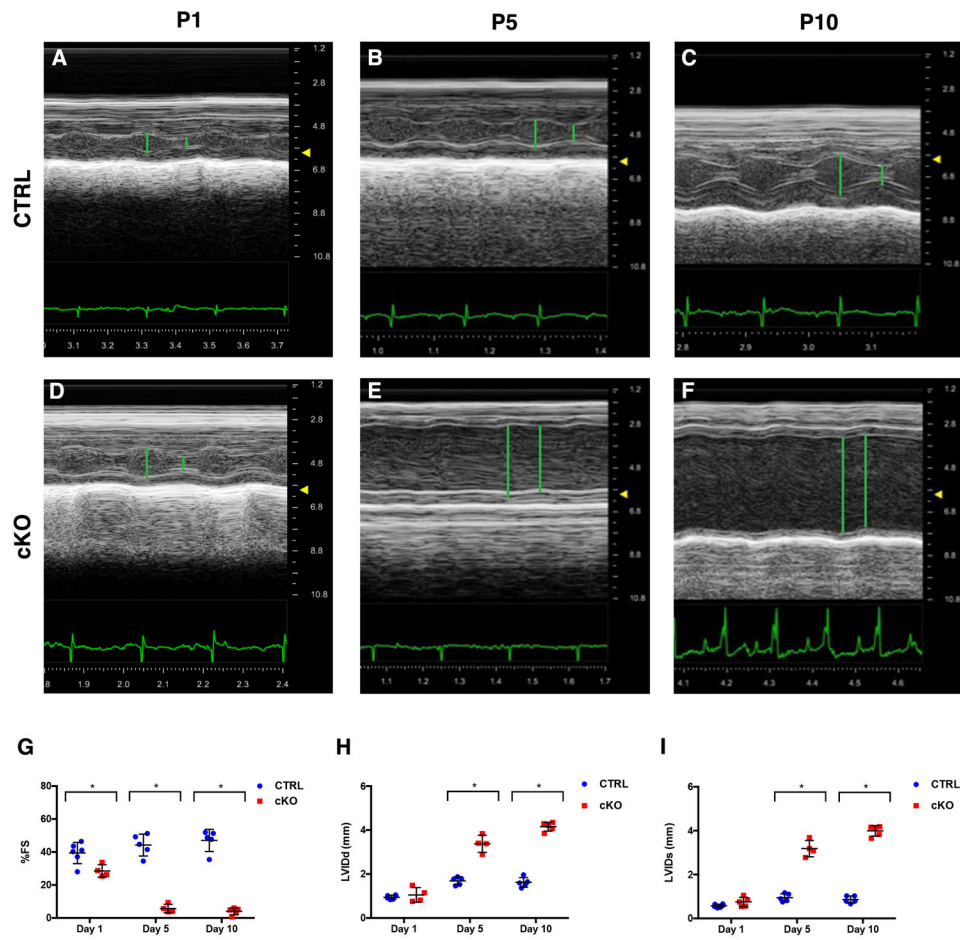


Figure 2. Cardiomyocytes-specific KO of NEXN results in reduced cardiac function. (A-F) Representative echocardiographic M-mode images of NEXN mice: (A) P1 CTRL, %FS 40, LVIDd 0.84mm, LVIDs 0.50mm, heart rate (HR) 297; (B) P5 CTRL, %FS 46, LVIDd 1.42mm, LVIDs 0.76mm, HR 455; (C) P10 CTRL, %FS 49, LVIDd 1.96mm, LVIDs 1.03mm, HR 484; (D) P1 cKO, %FS 25, LVIDd 1.15mm, LVIDs 0.81mm, HR 410; (E) P5 cKO, %FS 9, LVIDd 3.40mm, LVIDs 3.08mm, HR 492; (F) P10 cKO, %FS 5, LVIDd 4.29mm, LVIDs 4.14mm, HR 422. (G-I) graphs representing echocardiographic measurements from CTRL and cKO mice (n = 6-7 mice per time point): (G) % FS, (H) LVIDd and (I) LVIDs. Echocardiographic parameters reported in Supplemental Table 3. (*) Statistically significant differences with P value < 0.05.

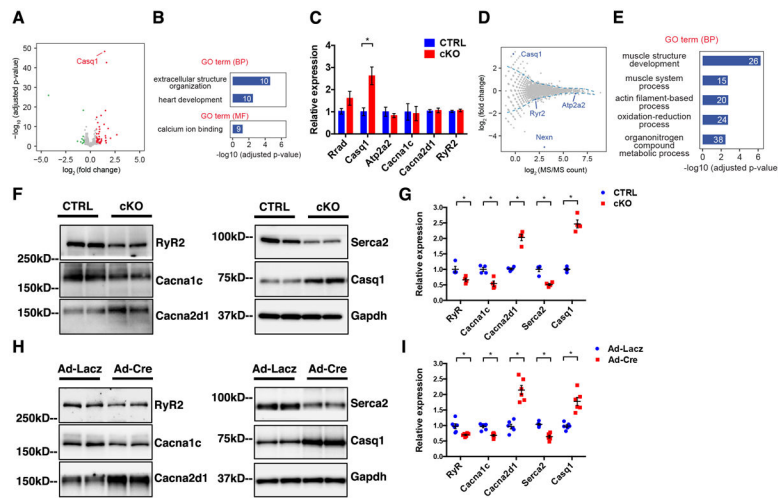


Figure 3. Abnormal expression of Ca²⁺-handling genes in NEXN cKO heart.

(A) Volcano plot of gene expression changes between CTRL and NEXN cKO P1 ventricles (n = 3). Genes with adjusted *P* value < 0.05 and fold change > 1.5 or < 2/3 are considered as significantly up- or down-regulated genes, and highlighted in red and green, respectively. (B) GO enrichment analysis of differentially expressed genes by RNAs-seq. Number of genes belonging to each category is indicated. BP: biological process, MF: molecular function. (C) qPCR analysis of Ca²⁺-handling genes from E18.5 mouse ventricles (n = 4). (D) MA plot showing the fold change of protein abundance against average MS/MS count assayed by mass spectrometry from P1 mouse ventricles (n = 4). Blue dotted line: fold-change cutoff selecting differentially expressed proteins. (E) GO enrichment analysis of differentially expressed proteins by mass spectrometry. (F-H) Western blot representative images and (G-I) quantification graphs of Ca²⁺-handling proteins from (F-G) E18.5 mouse ventricles (n = 4) and from (H-I) isolated neonatal NEXN^{f/f} cardiomyocytes treated with Ad-LacZ or Ad-cre virus (n=6). (*) Statistically significant differences with *P* value < 0.05.

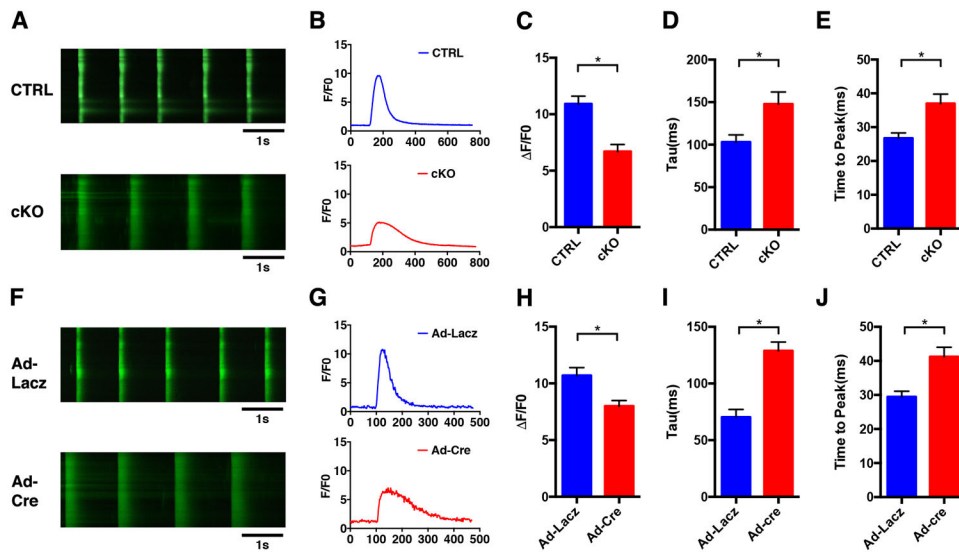


Figure 4. Alteration of Ca²⁺ dynamics in NEXN cKO cardiomyocytes.

(A) Representative time-lapse confocal images (scale bars 1 sec), Ca²⁺ transients measurements were performed at a pace of 0.5Hz; (B) representative Ca²⁺ transient curve; and (C-E) histograms showing results from quantifications of Ca²⁺ transient (C) amplitude (F/F₀) (D)transient decay (Tau) and (E) time to peak of live cardiomyocytes isolated from E18.5 CTRL and cKO ventricles were labeled with Fluo4 (n=6 mice). (F) Representative time-lapse confocal images (scale bars 1 sec); (G) representative Ca²⁺ transient curve and (G-J) histograms showing results from quantification of Ca²⁺ transient (H) F/F₀ and (I) Tau and (J) time to peak of E18.5 isolated neonatal cardiomyocytes *Nexn*^{f/f} treated with Ad-Lacz and Ad-cre virus labeled with Fluo4 (n=6 mice). (*) Statistically significant differences with P value < 0.05.

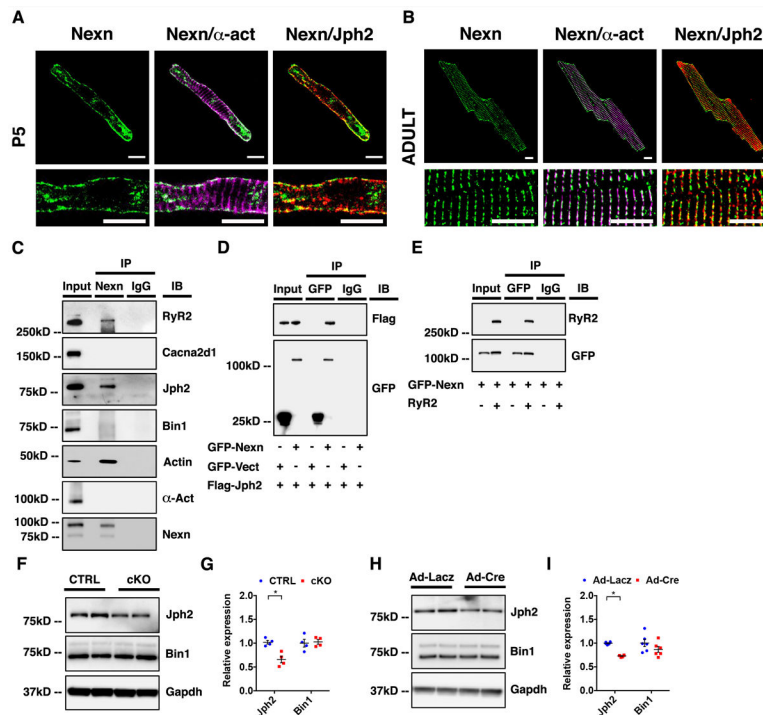


Figure 5. NEXN localizes to the JMC and interacts with junctional SR proteins.

(A) Representative confocal images of a P5 CTRL cardiomyocyte showing how NEXN in green do not co-localize with α -actinin (α -act) in magenta, while co-localizing with Jph2 in red; scale bars 10 μ m. (B) Representative confocal images of an adult CTRL cardiomyocyte in the lower panels showing dyadic localization of NEXN; scale bars 10 μ m. Fig (C) Co-immunoprecipitation of NEXN with putative binding partners using heart tissue lysates. (D) Immunoprecipitation of GFP-tagged NEXN and Flag-tagged Jph2 co-expressed in HEK293 cells. (E) Immunoprecipitation of GFP-tagged NEXN and tetracycline (10 μ g/ml, 24 hours) induced RyR2 co-expressed in a stable tetracycline inducible HEK293 cell line expressing RyR2. (F-H) Western blot representative images and (G-I) quantification graphs of Ca²⁺-handling proteins from (F-G) E18.5 mouse ventricles (n = 4) and from (H-I) isolated neonatal NEXN^{f/f} cardiomyocytes treated with Ad-LacZ or Ad-cre virus (n=6). (*) Statistically significant differences with P value < 0.05.

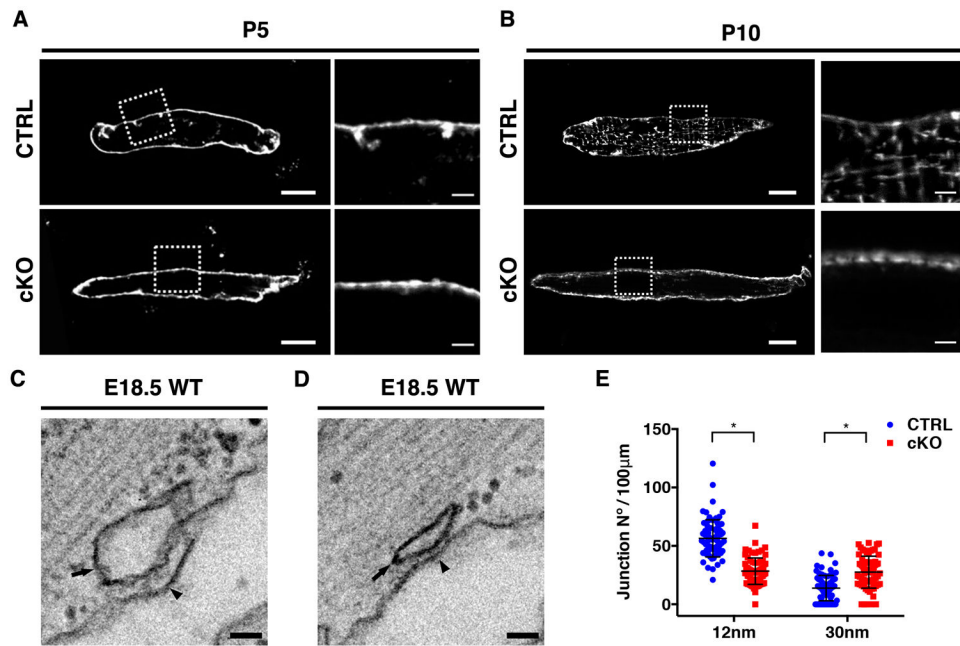


Figure 6. NEXN is indispensable for MCS stability and T-tubule formation.

(A-B) Representative live confocal images of (A) P5 and (B) P10 CTRL and *Nexn* cKO cardiomyocytes stained with Di-8 Anepps; low magnification scale bars 10 μm, high magnification scale bars 2 μm. (C-D) Representative electron microscopy (EM) images of E18.5 mouse heart ventricles showing the two different types of junctional complexes between the sarcolemma and the SR membrane with gap sizes of about (C) 12 and (D) 30 nm; scale bars 50 nm. (E) MCS occurrence quantification. Data were obtained from EM analysis of heart ventricle cardiomyocytes from *Nexn* cKOs and CTRLs E18.5 (n=3); for the *Nexn* cKO, 689 μm of sarcolemma length were analyzed; for the CTRL 876 μm of sarcolemma length were analyzed. (*) Statistically significant differences with P value < 0.05.

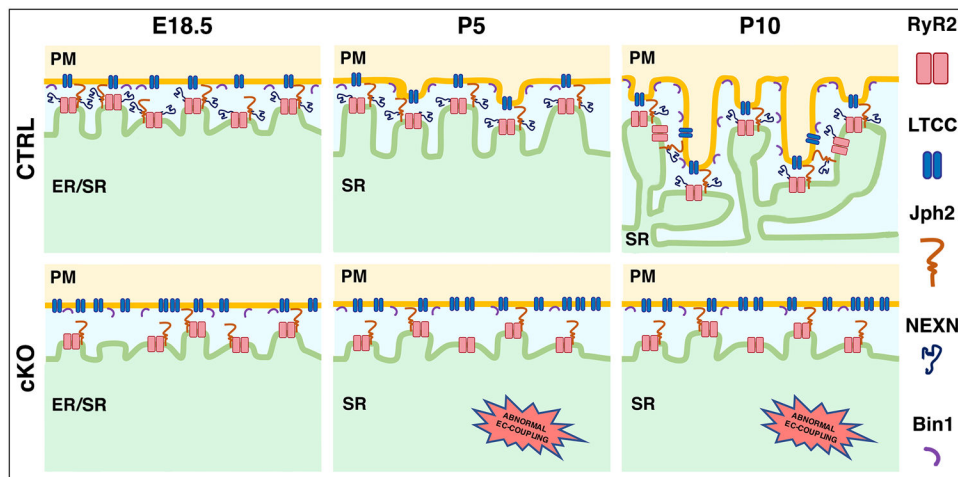


Figure 7. Model for NEXN role in cardiomyocytes.

At prenatal stage, NEXN is essential for the establishment of the JMCs. During neonatal stage (around P5), NEXN stabilization of the JMC allow the PM/SR tethering and PM buds start to invaginate inside the cell. Later in the development (around P10), the proper formation of JMCs leads to the deeper invagination of the forming T-tubules and the maturation of the dyads. Indeed, in cardiomyocytes lacking NEXN, the decrease of 12nm gap size junctions is observed. Furthermore, absence of NEXN prevent the sarcolemmal invaginations at P5 followed by a non-formation of T-tubules at P10. Finally, as a result of the altered membrane network, loss of NEXN in cardiomyocytes induce EC-coupling defects accompanied by severe DCM.